Neuron, Vol. 21, 1177–1188, November, 1998, Copyright ©1998 by Cell Press

# Submillisecond Kinetics of Glutamate Release from a Sensory Synapse

**Henrique von Gersdorff,[†§] Takeshi Sakaba,[*] Ken Berglund,[*] and Masao Tachibana[*‡]**
[*]Department of Psychology
Graduate School of Humanities and Sociology
The University of Tokyo
7–3–1 Hongo, Bunkyo-ku
Tokyo 113–0033
Japan
[†]Department of Membrane Biophysics
Max Planck Institute for Biophysical Chemistry
Am Fassberg
D-37077 Göttingen
Federal Republic of Germany

## Summary

**Exocytosis-mediated glutamate release from ribbon-type synaptic terminals of retinal bipolar cells was studied using AMPA receptors and simultaneous membrane capacitance measurements. Release onset (delay $<$0.8 ms) and offset were closely tied to $Ca^{2+}$ channel opening and closing. Asynchronous release was not copious and we estimate that there are $\sim$5 $Ca^{2+}$ channels per docked synaptic vesicle. Depending on $Ca^{2+}$ current amplitude, release occurred in a single fast bout or in two successive bouts with fast and slow onset kinetics. The second, slower bout may reflect a mobilization rate of reserve vesicles toward fusion sites that is accelerated by increasing $Ca^{2+}$ influx. Bipolar cell synaptic ribbons thus are remarkably versatile signal transducers, capable of transmitting rapidly changing sensory input, as well as sustained stimuli, due to their large pool of releasable vesicles.**

## Introduction

Fast and point-to-point neuronal communication is achieved by the rapid release of transmitter at active zones following the fusion of small clear core synaptic vesicles. Ribbon-type active zones are specialized structures that are widespread among sensory neurons, such as retinal bipolar cells, hair cells, electroreceptors, and photoreceptors. Interestingly, ribbon synapses can transmit a wide bandwidth of information at rates that greatly exceed those of conventional synapses (de Ruyter van Steveninck and Laughlin, 1996) and operate via graded membrane potential changes (Werblin and Dowling, 1969; Kaneko, 1970). At retinal bipolar cells, for example, these membrane potential changes can be very rapid or slow depending on the intensity and wavelength of light stimuli (Saito et al., 1979). Neurotransmitter release from the giant terminals of goldfish bipolar cells is triggered by the voltage-dependent opening of $Ca^{2+}$ channels (Tachibana et al., 1993), but the extent to which release precisely tracks the opening and closing of $Ca^{2+}$ channels remains a key unresolved issue.

In order to study the kinetics and capacity of release at bipolar cell synaptic terminals, two indirect experimental approaches have recently been employed. Using membrane capacitance as an index of net cell surface area (Neher and Marty, 1982), a saturable phasic mode of exocytosis has been suggested (von Gersdorff and Matthews, 1997; Sakaba et al., 1997b), whereas a continuous mode of exocytosis with high capacity has been reported with FM1-43 fluorescence (Lagnado et al., 1996). These measurements are, however, also sensitive to membrane turnover processes reflecting endocytosis (Smith and Betz, 1996) and thus unrelated to secretion, so it is important to couple them to the simultaneous detection of released molecules (Chow et al., 1996; Albillos et al., 1997; Moser and Neher, 1997). In addition, secretion and membrane area changes due to exocytosis may not correlate well if vesicles are partially filled with transmitter (Cousin and Nicholls, 1997; Song et al., 1997) to varying degrees (e.g., the extreme case of empty vesicles fusing with the plasma membrane will produce capacitance jumps, but no transmitter release).

Previously, due to their high affinity for glutamate, N-methyl-D-aspartate (NMDA) receptors have been used (Copenhagen and Jahr, 1989; Tachibana et al., 1993) to monitor release, although they are slow to activate and deactivate and thus may not faithfully track successive bouts of rapid release. $\alpha$-amino-3-hydroxy-5-methyl-4-isoxazolepropionic acid (AMPA) receptors, on the other hand, are extremely fast but have a low affinity for glutamate and desensitize quickly (Trussell and Fischbach, 1989). Cyclothiazide (CTZ), however, reduces AMPA but not kainate (Partin et al., 1993) receptor desensitization, while increasing its affinity for glutamate (Yamada and Tang, 1993). Indeed, fast application of glutamate onto membrane patches from catfish horizontal cells elicits currents that desensitize fully within 2–3 ms, and 100 $\mu$M CTZ completely abolishes this desensitization (Eliasof and Jahr, 1997). Catfish horizontal cells express a high density of AMPA receptors (Eliasof and Jahr, 1997), and we thus used these AMPA receptors treated with CTZ to detect fast glutamate release and simultaneously measured time-resolved membrane capacitance to monitor depolarization-evoked exocytosis of synaptic vesicles.

Using the integral of the AMPA receptor–mediated currents as a measure of glutamate release, we find that capacitance jumps are highly correlated with release. Two saturable components of release are sequentially evoked by long depolarizations. The first component is very fast and phasic, presumably due to the rapid fusion and depletion of a pool of docked vesicles (Heuser and Reese, 1981). The second component has slower kinetics that may reflect the mobilization rate of vesicles from a reserve pool to their fusion sites (von Rüden and Neher, 1993; Steyer et al., 1997). However, asynchronous release (Barrett and Stevens, 1972; Gleason et al., 1994)

[‡]To whom correspondence should be addressed (e-mail: ltmasao@hongo.ecc.u-tokyo.ac.jp).
[§]Present address: Vollum Institute, Oregon Health Sciences University L−474, 3181 S. W. Sam Jackson Park Road, Portland, Oregon 97201.

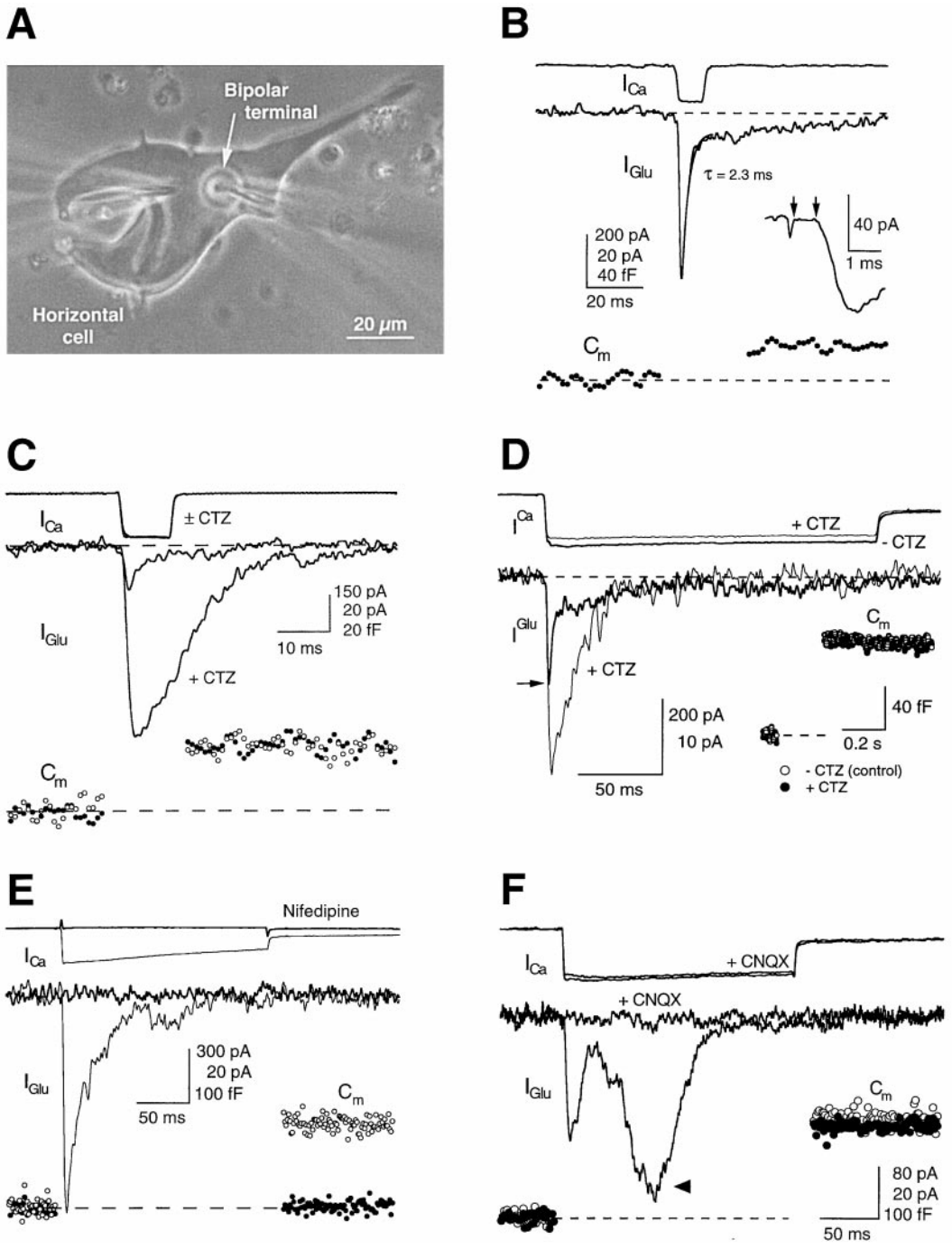


Figure 1. Simultaneous Measurement of Glutamate Release and Membrane Capacitance

(A) Phase-contrast photograph of a goldfish bipolar cell terminal held by a patch pipette (right) and pressed against the surface of a catfish horizontal cell, which is being recorded from via a second patch pipette (left).

(B) Simultaneous recording of bipolar terminal $I_{Ca}$, $C_m$, and horizontal cell $I_{Glu}$ (same time scale). $I_{Ca}$ was elicited by a voltage-clamp step depolarization from −60 mV to −10 mV for 10 ms. The initial decay phase of $I_{Glu}$ was best fit by a single exponential ($\tau = 2.3$ ms; superimposed on the data). The horizontal cell holding potential was −50 mV. The inset shows the average of four successive responses elicited at 30–40 s time intervals. Due to the close association between the two cells, a capacitative transient was induced in the horizontal cell current by the abrupt voltage change in the bipolar terminal. The arrows mark the end of the capacitative transient (start of $I_{Ca}$) and beginning of $I_{Glu}$. The external solution contained no CTZ or D-AP5.

(C) Superimposed responses evoked by two 10 ms pulses to −10 mV without (upper trace) and with 100 μM CTZ in the external solution (lower trace). Both responses are in the presence of 50 μM D-AP5. CTZ increased the amplitude (4-fold) and slowed the decay of $I_{Glu}$, but had no effect on $I_{Ca}$ or $C_m$ (open circles, control; closed circles, CTZ).

(D) Same as (C) but with 200 ms pulses to −10 mV without and with 100 μM CTZ in the external solution, which contained 50 μM D-AP5. In

after $Ca^{2+}$ channel closure was not copious and decayed sharply within ~300 ms or less, depending on the amount of calcium influx. This rapid onset and termination of evoked release at a particular class of bipolar cell (ON-type Mb1; Sherry and Yazulla, 1993) may allow them to transmit high frequency signals with minimal distortion and filtering. Bipolar cell ribbon synapses thus have several properties in common with conventional action potential–driven synapses but also some remarkable differences, such as the appearance of a large second component of release during sustained stimulation. Depending on the degree and extent of depolarization, these properties may permit them to function in both phasic (high output) and/or more sustained (low output) secretory modes, setting the bipolar cell synaptic ribbon apart from the photoreceptor ribbon (Rieke and Schwartz, 1996), which is thought to release in an exclusively tonic manner.

## Results

### Simultaneous Glutamate Release and Capacitance Measurements

Freshly dissociated goldfish Mb1 bipolar terminals (Tachibana et al., 1993) were whole-cell patch clamped and the pipette, with attached terminal, was lifted above the recording chamber bottom. A cultured catfish horizontal cell was next whole-cell patch clamped. The bipolar terminal was then lowered and pressed against the surface of the horizontal cell (Figure 1A). Constant perfusion of the cell pair was then initiated. A 10 ms step depolarization to −10 mV elicited a calcium current ($I_{Ca}$) and a capacitance jump ($C_m$) in the bipolar terminal and an excitatory glutamate-induced current ($I_{Glu}$) in the horizontal cell (Figure 1B). $I_{Glu}$ disappeared when the cells were not tightly juxtaposed against each other. The inset in Figure 1B shows the fast rise time of $I_{Glu}$ (10%–90% = 0.76 ms, mean ± SD = 1.0 ± 0.3 ms, N = 20), consistent with rapid delivery of glutamate. The delay between the bipolar depolarization and the start of $I_{Glu}$ was 0.8 ms (inset arrows), similar to frog neuromuscular junction (Katz and Miledi, 1965; Yazejian et al., 1997). If the cell-pair gap is <0.5 μm, a likely case given that we pressed the cells together, diffusion should contribute <0.1 ms to this delay. The decay phase of $I_{Glu}$ was best fit by two exponentials with time constants $\tau_1$ = 1.8 ± 0.6 ms (N = 20, 81% of amplitude) and $\tau_2$ = 32 ± 26 ms with 50 μM D-AP5 (an NMDA receptor antagonist) present and the horizontal cell held at −60 or −70 mV.

Similar to its effect on excitatory postsynaptic currents (EPSCs) of hippocampal (Diamond and Jahr, 1995) and retinal ganglion cells (Lukasiewicz et al., 1995), 100 μM CTZ enhanced 1.7- to 4-fold the amplitude of $I_{Glu}$ and slowed its decay (single exponential fit, $\tau_{CTZ}$ = 14 ± 4.6 ms; 10%–90% rise time, 2.2 ± 0.6 ms; N = 21; Figures 1C and 1D). CTZ slows the decay of quantal or mini EPSCs (Yamada and Tang, 1993). The slower decay of $I_{Glu}$ probably reflects this, as well as continued quantal release of transmitter, since the time course of deactivation of our CTZ-treated AMPA receptors upon sudden removal of glutamate is very fast (1–2 ms; Eliasof and Jahr, 1997). Continued quantal release shapes the decay phase of AMPA EPSCs at some fast CNS synapses (Diamond and Jahr, 1995; Isaacson and Walmsley, 1995). However, in spite of the local and rapid superfusion of the cell pair, we cannot rule out some contribution from glutamate diffusion. CTZ also slightly reduced the amplitude of $I_{Ca}$ (range 0%–14%, average 8%), but this small effect did not alter $C_m$ elicited by either 10 or 200 ms pulses to −10 mV (N = 21; Figures 1C and 1D), probably because calcium current amplitude still remained above 120 pA, where it already elicits saturating capacitance jumps (see Figure 1 of von Gersdorff and Matthews, 1997). Thus, contrary to results at hippocampal synapses (Diamond and Jahr, 1995), CTZ does not seem to directly affect the release machinery at bipolar terminals. The L-type $Ca^{2+}$ channel antagonist nifedipine (100 μM) abolished completely $I_{Ca}$, $I_{Glu}$, and $C_m$ (N = 5; Figure 1E), while 10 μM CNQX, an AMPA/kainate receptor antagonist, blocked $I_{Glu}$ completely but had no significant effect on $I_{Ca}$ or $C_m$ (N = 9; Figure 1F). $I_{Glu}$ is thus an AMPA receptor–mediated current activated by rapid glutamate release from bipolar terminals.

### Two Components of Release

Figure 1F illustrates in addition a surprising feature of release from ribbon-type synaptic terminals, namely its biphasic nature. Using NMDA receptors as glutamate detectors, two components of release were also clearly detected (Sakaba et al., 1997b). The first component of release was shown to be resistant to high concentrations of $Ca^{2+}$ buffer (5 mM EGTA), while the appearance of the second component could be delayed by as much as 1–2 s in 5 mM EGTA–loaded terminals. However, the kinetics of the release process was greatly filtered by the slow activation and deactivation rates of NMDA receptors (Lester et al., 1990). The speed of AMPA receptors, combined with the treatment with CTZ, allowed us to monitor the kinetics of the two components of release, and moreover to also use physiological amounts of internal $Ca^{2+}$ buffer (0.2 mM BAPTA; see von Gersdorff and Matthews, 1997) within the bipolar terminals. The kinetics of the release process was thereby distorted to a minimum degree.

As shown in Figure 1F, the first component of release has a fast onset, triggered by activation of $I_{Ca}$, while

this example, CTZ increased the amplitude (1.7-fold) and slowed the decay of $I_{Glu}$ and decreased the amplitude of $I_{Ca}$ (14%); however, this did not affect $C_m$. The horizontal cell was held at −60 mV.

(E) Superimposed responses evoked by two 200 ms pulses to −10 mV, without and with 100 μM nifedipine in the external solution. The leak current observed after repolarization is a $Ca^{2+}$-dependent $Cl^-$ current that is present whenever long pulses elicit a large $I_{Ca}$ (Okada et al., 1995). The horizontal cell was held at −50 mV. $C_m$: open circles, control; closed circles, nifedipine.

(F) Superimposed responses evoked by two 200 ms pulses to −10 mV without and with 10 μM CNQX in the external solution. The arrowhead indicates the second component of release. $C_m$: open circles, control; closed circles, CNQX.

The external solution in (E) and (F) contained 100 μM CTZ and 50 μM D-AP5.

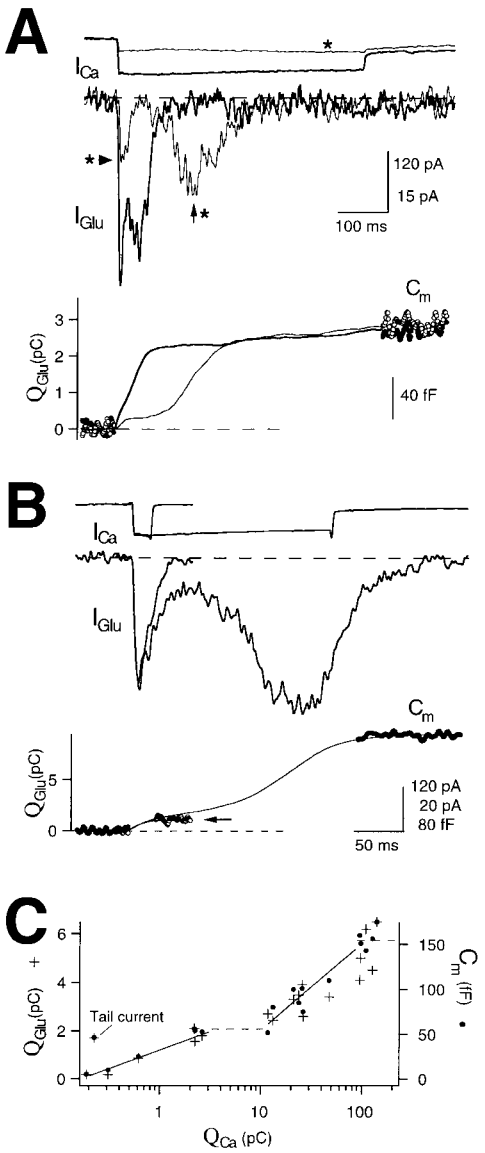


Figure 2. Correlation between $Q_{Glu}$ and $C_m$

(A) Superimposed responses evoked by 500 ms pulses to −30 mV (asterisk) and to −10 mV. The bottom panel shows the integral of $I_{Glu}$ ($I_{Glu}$ charge or $Q_{Glu}$) and the corresponding $C_m$ (open circles, −10 mV pulse; closed circles, −30 mV pulse) on the same time scale. The arrowhead and vertical arrow show the peak of the first and second components of release elicited by the −30 mV pulse, respectively.

(B) Superimposed responses evoked by 20 and 200 ms pulses to −10 mV. The arrow in the bottom panel indicates the peak $Q_{Glu}$ of the 20 ms pulse (obscured by the superimposed $C_m$).

(C) An example of a cell pair where simultaneously measured $Q_{Glu}$ (pluses) and $C_m$ (closed circles) are plotted as a function of the integral of $I_{Ca}$ ($Q_{Ca}$).

In (A), (B), and (C), the zero level $Q_{Glu}$ and baseline capacitance were aligned, and the peak $Q_{Glu}$ and peak $C_m$ were normalized.

the second component (arrowhead) has a much slower onset. The prominence of the second component depended on $I_{Ca}$ per unit area. For an influx of <50 pA/pF (N = 16; e.g., Figure 1F), the second component is temporally separated from the first component, whereas for an influx of >50 pA/pF (N = 18; e.g., Figures 1D and 1E), the first and second components fuse together into a single rapid bout of glutamate release, as probably also occurs in caged $Ca^{2+}$ flash photolysis experiments (Heidelberger, 1998). This is illustrated in Figure 2A, where $I_{Ca}$ and $I_{Glu}$ elicited from the same cell pair by two successive 500 ms step depolarizations, one to −30 mV (asterisk) and another to −10 mV, are superimposed. The −30 mV pulse elicited an $I_{Glu}$ that had a second component (arrow and asterisk) that peaked later than the second component of the −10 mV pulse. $C_m$ and the integral of $I_{Glu}$ ($Q_{Glu}$) were, however, approximately the same as indicated by the lower panel, consistent with vesicle pool depletion (Elmquist and Quastel, 1965; Liu and Tsien, 1995; Rosenmund and Stevens, 1996).

In a few cell pairs (N = 3), the second component of release was clearly detected without CTZ treatment. The very rapid recovery from desensitization of the particular AMPA receptor subtype expressed in catfish horizontal cells (recovery time constant $\tau$ = 8 ms; Eliasof and Jahr, 1997) thus may allow them to respond to the second component of release. In most instances, however, the second component of release was not detectable without CTZ treatment, either because the $Ca^{2+}$ influx was >50 pA/pF, or because the second component of release started while some residual glutamate from the first component was still present, thus maintaining many AMPA receptors in a desensitized state (Trussell and Fischbach, 1989). In the intact retina, where glutamate transporters may rapidly buffer glutamate concentrations after the first component of release, it is possible that the second component plays an important role in sustaining postsynaptic action potential firing.

### Relationship between $C_m$ Changes and Glutamate Release

We next asked how well capacitance and glutamate release measurements agreed, taking $Q_{Glu}$ as an index of exocytosis. Figure 2B shows an example where two successive $I_{Ca}$ elicited in the same bipolar terminal by pulses to −10 mV for 20 ms and 200 ms are superimposed. The lower panel shows that normalizing the capacitance jump elicited by the 200 ms pulse with the corresponding $Q_{Glu}$ accurately predicts the 20 ms pulse $C_m$ and $Q_{Glu}$ amplitude (arrow). Figure 2C shows another example cell pair with multiple responses (coefficient of variance of the peak $I_{Glu}$: CV = 0.072 for 14 responses to −10 mV pulses elicited during 13 min of recording). Note that the increase in $C_m$ and $Q_{Glu}$ with $Q_{Ca}$ (integral of $I_{Ca}$) has two different slopes and two plateau regions: one corresponding to 5–20 ms pulses, and another to pulses of >200 ms (Mennerick and Matthews, 1996; Sakaba et al., 1997b). We see that $C_m$ and $Q_{Glu}$ are highly correlated across three orders of magnitude of $Ca^{2+}$ influx. Similar plots were obtained for eight cell pairs (average correlation coefficient between $C_m$ and $Q_{Glu}$ = 0.96 ± 0.14). This result indicates that $C_m$ jumps reflect exocytosis, and not the balance of simultaneous exo- and endocytosis.

Notice also that in Figure 2C the response to a $Ca^{2+}$ tail current evoked by a 10 ms pulse to +60 mV ($C_m$ = 46 fF and $Q_{Ca}$ = 0.23 pC) was more effective at triggering

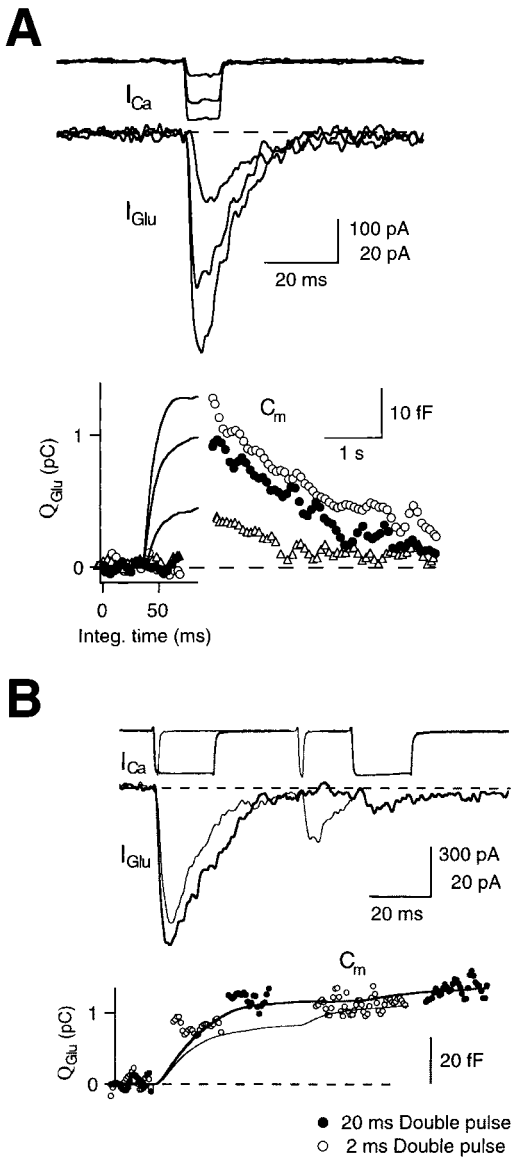


Figure 3. Fast Endocytosis and Paired-Pulse Depression

(A) Superimposed responses evoked by 10 ms pulses to −30, −20, and −10 mV that elicited respectively larger $I_{Ca}$ and $I_{Glu}$, as well as peak $Q_{Glu}$ and $C_m$ responses (lower panel). The open circle (−10 mV), closed circle (−20 mV), and open triangle (−30 mV) symbols show the $C_m$ jump and decay back to baseline capacitance (note the different time scales between panels). Peak $Q_{Glu}$ and peak $C_m$ are normalized so that their values coincide. $Q_{Glu}$ is plotted as a function of integration time.

(B) Superimposed responses evoked by double pulses of 2 ms (thin traces) and 20 ms (thick traces) duration to −10 mV, with an interpulse interval of 45 ms. $I_{Ca}$ was filtered at 1 kHz and $I_{Glu}$ at 350 Hz. The horizontal cell was held at −50 mV.

release than the response to a 10 ms pulse to −30 mV ($C_m$ = 25 fF and $Q_{Ca}$ = 0.62 pC). This is probably due to the faster activation and larger amplitude of $I_{Ca}$ (670 pA) for the brief $Ca^{2+}$ tail current than for the much longer but smaller amplitude $I_{Ca}$ (65 pA) elicited by the pulse to −30 mV. Thus, the amplitude of $I_{Ca}$ seems to control release more effectively than the integral of $I_{Ca}$ (Spencer et al., 1989; Augustine, 1990), in line with a low affinity $Ca^{2+}$ sensor triggering the release of the first component.

### Fast Endocytosis Does Not Overlap with Exocytosis

Following evoked $C_m$ jumps to an elevated value, capacitance relaxes back to baseline, due presumably to endocytosis of fused synaptic vesicle membrane (De Camilli and Takei, 1996). This is illustrated in Figure 3A, where responses to 10 ms voltage-clamp pulses at different potentials are shown, but now with $C_m$ monitored on a longer time scale so as to display its recovery back to baseline. Peak $Q_{Glu}$ again coincides remarkably well with the respective $C_m$ jumps (lower panel of Figure 3A), which increase in magnitude as $I_{Ca}$ increases in amplitude. $C_m$ recovery could be fit by single exponentials with similar time constants ($\tau_{endo}$ = 0.9, 1.8, and 1.5 s for the −30, −20, and −10 mV pulses, respectively), indicating that the rate of capacitance recovery (endocytosis) did not depend on the amount of previous exocytosis (Ryan et al., 1996) for these short 10 ms pulses, and that CTZ does not affect this rate since in its absence $C_m$ also recovers with time constants of 1–2 s (von Gersdorff and Matthews, 1997). However, longer depolarizations (pulses of >250 ms) lead to slower rates of endocytosis in bipolar cell terminals, as occurs also in the frog neuromuscular junction (Wu and Betz, 1996). In Figure 3A, $I_{Glu}$ decays with a $\tau_{CTZ}$ of 9.8 ms, so the rate of recovery of capacitance should not be contaminated by ongoing release. Exocytosis and endocytosis are thus temporally well separated for bipolar terminals, since the rate of endocytosis is at least 100-fold slower than that of the first component of exocytosis.

### Paired-Pulse Depression

The lack of asynchronous release after the first component of release has been elicited by 10 ms pulses may be due to the depletion of a readily releasable pool of vesicles. Indeed, a rapid component of $C_m$ jump has been shown to saturate for 5–20 ms pulses (Mennerick and Matthews, 1996). Consistent with this $C_m$ saturation, we find that both the amplitude and integral of $I_{Glu}$ are not significantly different for single 5 and 10 ms pulses to −10 mV (N = 8). Figure 3B shows a paired-pulse experiment where we have simultaneously monitored $C_m$ and $I_{Glu}$ changes. The first component of glutamate release was elicited by a 20 ms pulse to −10 mV and then, 40 ms later, by a second 20 ms pulse. Notice that both 20 ms pulses elicited almost identical $I_{Ca}$ (the second $I_{Ca}$ had a facilitated amplitude of 4%, N = 14), but the second 20 ms pulse elicited very little release and $C_m$ jump. By contrast, 30 s later in the same cell pair, a 2 ms pulse to −10 mV elicited a smaller $I_{Glu}$ (and proportionally smaller $Q_{Glu}$ and $C_m$ jump) than the 20 ms pulse. However, a second 2 ms pulse given 40 ms later elicited a clear amount of release and a $C_m$ jump. Notice that the final level of $Q_{Glu}$ and $C_m$ reached by the second 2 ms pulse was almost the same as that reached by the first 20 ms pulse. Thus, the first component of release is saturated by a 20 ms pulse to −10 mV but not by a single 2 ms pulse. The first component of release thus

displays pronounced paired-pulse depression (Mennerick and Zorumski, 1995; Stevens and Wang, 1995).

### Depolarization-Dependent Delays in Release

In order to study the delay in release, Figure 4A shows an example where successive $I_{Ca}$ elicited by pulses to different potentials are superimposed. The peak $I_{Ca}$ and $I_{Glu}$ occur for the −10 mV pulse, while the +60 mV pulse (shown in bold) elicits release only during the transient $Ca^{2+}$ tail current. These results are very similar to studies of depolarization–release coupling in the squid giant synapse, which contains conventional active zones (Llinás et al., 1981; Augustine et al., 1985), and the large off response elicited by the +60 mV pulse was also observed in paired recordings from rat cerebellar slices (see Figure 8 of Vincent and Marty, 1996). Notice that the delay between the bipolar cell voltage-clamp pulse and the start of $I_{Glu}$ increases as the depolarizing pulse amplitude decreased from −10 to −37 mV. The arrows indicate that the delay for the −37 mV pulse is quite long (4.5 ms) due to the slow activation and small amplitude of $I_{Ca}$. These results also directly demonstrate a steep "synaptic gain" for the bipolar terminal in its operating range from −40 mV to −20 mV.

Figure 4B shows that the strikingly fast tail $I_{Ca}$ is very effective in triggering an $I_{Glu}$ with a short delay. The delay defined as from the peak rate of rise of $I_{Ca}$ (first hatched line) to the point where an exponential fit to the integral of $I_{Glu}$ contacts the baseline (second hatched line) is 1.1 ms (1.2 ± 0.3 ms, N = 5). This definition of delay is similar to that used in flash photolysis of caged $Ca^{2+}$ experiments (Heidelberger et al., 1994), where a delay of 1 ms corresponded to a $[Ca]_i$ at the fusion site of ~100 μM. Likewise, a transient rise of $[Ca]_i$ to ~75 μM at the fusion site triggers phasic release at the crayfish neuromuscular junction (Lando and Zucker, 1994). Such large $[Ca]_i$ can only be found near the mouth of open $Ca^{2+}$ channels, which must thus lie within <50 nm from fusion sites (Simon and Llinás, 1985; Zucker and Fogelson, 1986; Naraghi and Neher, 1997).

### How Many $Ca^{2+}$ Channels Does It Take to Fuse One Vesicle?

A fundamental question in synaptic transmission is how many open $Ca^{2+}$ channels are necessary for the triggering of one synaptic vesicle fusion (Augustine, 1990; Stanley, 1993; Neher, 1998). The answer may vary from synapse to synapse and depends partly on the distance between $Ca^{2+}$ channels and release sites. To address this, we estimated the total number of functional $Ca^{2+}$ channels on the terminal by eliciting $Ca^{2+}$ tail currents in the presence of Bay K 8644, a L-type $Ca^{2+}$ channel agonist (Nowycky et al., 1985) that increases the open probability without affecting the single channel current amplitude (Fox et al., 1987). In chick sensory neurons, the open probability of single L-type $Ca^{2+}$ channels increases steeply with depolarization, reaching a value of 0.5 at +30 mV (Fox et al., 1987). We elicited tail currents with 10 ms voltage-clamp pulses from −60 to +60 mV. The peak tail $I_{Ca}$ amplitude (412 ± 150 pA, N = 19, $C_m$ = 21 ± 16 fF) was increased 2.6-fold by 5–10 μM Bay K 8644, which also increased $C_m$ 2.4-fold. The ratio of the peak tail $I_{Ca}$ in Bay K 8644 to the single channel (Church

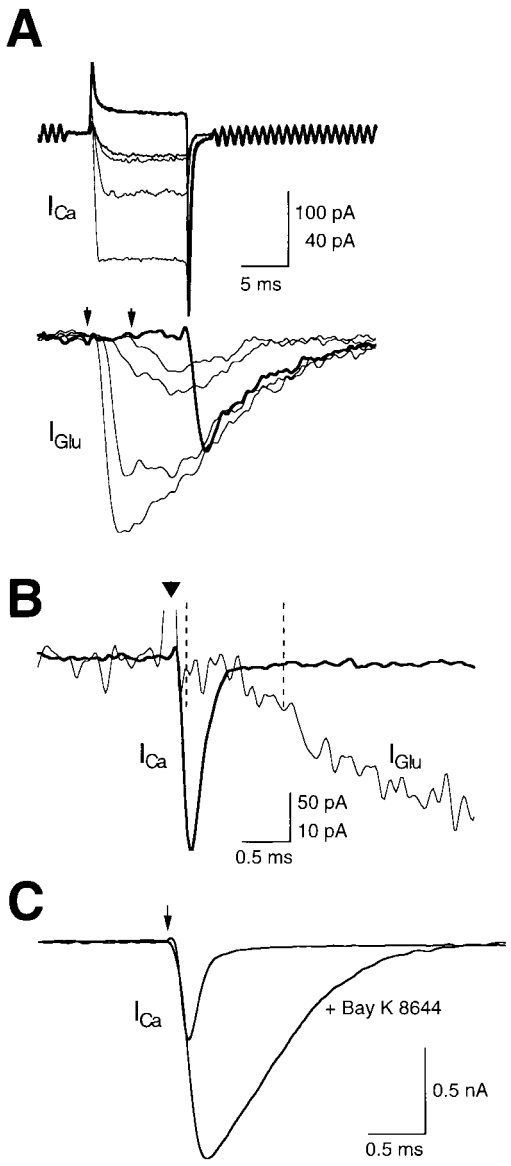


Figure 4. Submillisecond Glutamate Release Kinetics and Synaptic Delay

(A) Superimposed responses evoked by 10 ms pulses to +60 (in bold), −37, −35, −30 and −10 mV (from top to bottom) that elicited respectively larger $I_{Ca}$ and $I_{Glu}$, except for the $I_{Glu}$ response to the +60 mV pulse (in bold), which occurred only during the repolarization from +60 mV to −60 mV, when a tail $I_{Ca}$ is elicited. $I_{Ca}$ was filtered at 5 kHz to clearly display its activation kinetics, and as a consequence the sine wave imposed on the bipolar terminal to measure capacitance is not filtered out. $I_{Glu}$ was filtered at 350 Hz.

(B) Tail $I_{Ca}$ and corresponding $I_{Glu}$ evoked by a repolarization of the bipolar terminal from +60 to −60 mV (filtered at 5 kHz). The arrowhead marks the capacitative transient induced in the horizontal cell by the abrupt voltage change (120 mV) in the bipolar terminal. The vertical dashed lines indicate the delay in release (1.1 ms) between the peak derivative of $I_{Ca}$ and the point where an exponential fit to the integral of $I_{Glu}$ contacts the baseline. The amplitude of $I_{Ca}$ is 210 pA, and $\tau_{decay}$ = 120 μs (see Mennerick and Matthews, 1996).

(C) Tail $I_{Ca}$ without and with 5 μM Bay K 8644 in the external solution (no CTZ or D-AP5). The arrow marks the point where the bipolar terminal was repolarized from +60 to −60 mV. The amplitude of $I_{Ca}$ was increased 2.3-fold with Bay K 8644 treatment.

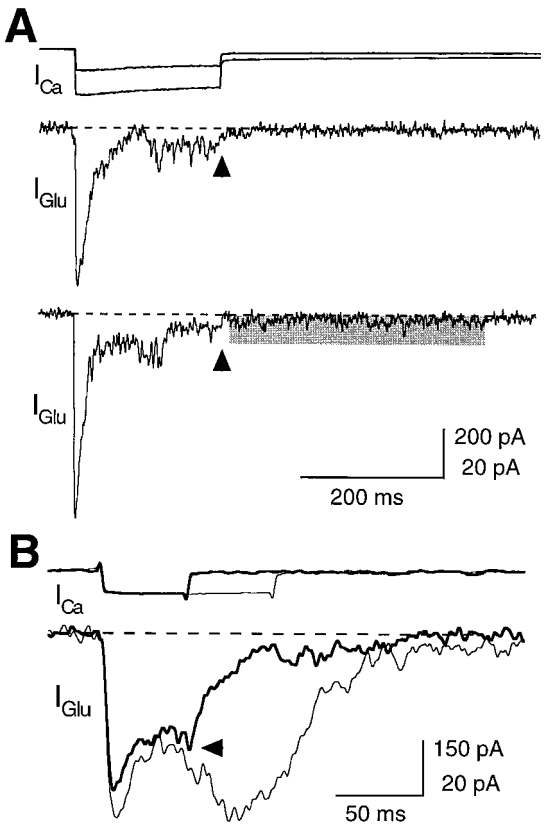


Figure 5. Extent of Asynchronous Release after $Ca^{2+}$ Channel Closure

(A) $I_{Ca}$ and $I_{Glu}$ responses evoked by 200 ms pulses to −30 mV and −10 mV that elicited, respectively, the second and third lower $I_{Glu}$ traces. $I_{Ca}$ amplitude was 86 and 185 pA for the −30 and −10 mV pulses, respectively. Clear asynchronous release is not observed after the −30 mV pulse; however, after the −10 mV pulse some asynchronous release was detected (shaded area). The bipolar terminal leak current observed after the −10 mV pulse is a $Ca^{2+}$-dependent $Cl^-$ current (see Figure 1E) and indicates that basal $[Ca]_i$ was elevated during this period.

(B) Responses evoked by 50 ms and 100 ms pulses to −10 mV that elicited, respectively, the bold and thin $I_{Glu}$ traces. The arrowhead marks the truncated second component of release evoked by the 50 ms pulse.

and Stanley, 1996) current (0.25 pA at −60 mV in 2 mM $Ca^{2+}$) gives, then, a good estimate of the number of channels, if we assume that nearly all $Ca^{2+}$ channels are open at the peak tail current. For the terminal of Figure 4C (peak $I_{Ca}$ = 1.3 nA), we thus estimate a total of at least 5200 $Ca^{2+}$ channels. Given its resting capacitance (3.5 pF), it should have ~1400 docked vesicles (von Gersdorff et al., 1996), making for an average of 3.7 $Ca^{2+}$ channels per docked vesicle. If we assume that the open probability, even under the above conditions, is still between 0.5 and 0.75, we then estimate that 5–7 functional $Ca^{2+}$ channels are closely associated with a docked vesicle, and stochastically open (Fox et al., 1987) at our standard depolarization of −10 mV to trigger its fusion.

### Asynchronous Release

We next addressed the issue of asynchronous release, defined as release following $Ca^{2+}$ current termination (Gleason et al., 1994; Goda and Stevens, 1994). Asynchronous release may be a major component of release at ribbon synapses (Lagnado et al., 1996; Rieke and Schwartz, 1996), if the calcium sensor for vesicle fusion has a high affinity for $Ca^{2+}$ (Goda and Stevens, 1994; Henkel and Almers, 1996). Figure 5A shows an example where depolarization to −30 mV for 200 ms elicited a response (upper panel) that had no detectable release after $I_{Ca}$ was terminated (arrowhead). However, a pulse to −10 mV elicited a larger $I_{Ca}$, significantly more release, and clear asynchronous release events (shaded area). The integral of the shaded area was about 11% of the total $I_{Glu}$ charge during $I_{Ca}$ activation, and plateaued within the first 300 ms after $I_{Ca}$ termination. Asynchronous release decayed sharply in <300 ms for 14 bipolar terminals with leak currents <30 pA at −60 mV. Thus, bipolar ribbon synapses do exhibit some degree of asynchronous release—however, not to the copious extent seen at some synapses (Gleason et al., 1994). This implies that for times >300 ms the recovery of capacitance back to baseline should reflect only endocytosis, since it is not contaminated by ongoing exocytosis. Major release was also quickly terminated by $I_{Ca}$ shutdown. Figure 5B shows an example of superimposed responses to pulses of 50 and 100 ms. Notice that the $I_{Glu}$ evoked by the 50 ms pulse (bold) was just beginning to display the second component (arrowhead) when it was abruptly interrupted by the sudden closure of $I_{Ca}$. The thinner $I_{Glu}$ trace shows that for the longer 100 ms pulse the second component of release is now successfully launched. This indicates that for the full activation of the second component of release sustained $Ca^{2+}$ influx is necessary. Moreover, the fast decay of $I_{Glu}$ after the end of the 50 ms pulse further suggests that slow diffusion of glutamate is not involved in generating the second component of release.

### Recovery from Depression

Finally, we investigated the time course of recovery from depression of the two components of glutamate release. Paired-pulse experiments with 200 ms pulses from −60 mV to −10 mV indicated no significant release for the second pulse when the interpulse interval was 125 ms (asterisk, Figure 6; N = 5); however, for interpulse intervals of 1 s, a clear detectable amount of release was observed that had a fast rise time (Figure 6). This indicates that the first component of release already recovers partially during a 1 s waiting period (Mennerick and Matthews, 1996), while the second component takes a longer time. Full recovery of both components of release was obtained with an interpulse interval of 20–30 s, in agreement with previous measurements of recovery from depression using NMDA receptor–mediated responses elicited by 1 s pulses ($\tau_{recovery}$ = 6.4 s; Sakaba et al., 1997b) and capacitance jumps elicited by 250 ms pulses ($\tau_{recovery}$ = 7.6 s; von Gersdorff and Matthews, 1997). Recovery from depression is dependent on Mg-ATP, and "cross-depletion" experiments with caged $Ca^{2+}$ flash photolysis support the hypothesis that depression is due to vesicle pool depletion (Heidelberger, 1998).

### Discussion

Employing AMPA receptors as detectors, we have shown that, when strongly depolarized, bipolar cell terminals

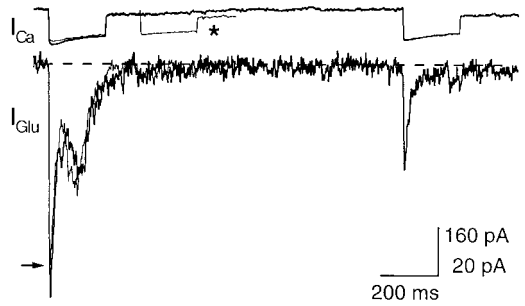


Figure 6. Recovery from Depression

Superimposed $I_{Ca}$ and $I_{Glu}$ responses evoked by two successive 200 ms pulses with interpulse intervals of 125 ms (thin traces) and 1 s (thick traces). The bipolar cell was depolarized from −60 mV to −10 mV. The horizontal cell was held at −70 mV. Responses were filtered at 100 Hz. The arrow marks the peak response elicited by the first 200 ms pulse, which was followed by a second pulse 125 ms later (asterisk) that elicited no clearly detectable amount of release.

are capable of releasing glutamate in a fast phasic mode akin to conventional CNS synapses (Sabatini and Regehr, 1996; Geiger et al., 1997). During sustained depolarizations, a slower and more extended mode of release (second component) occurs that can last for tens of milliseconds. Both of these modes are saturable, and their relative importance depends on the degree and extent of depolarization. Previous capacitance (Mennerick and Matthews, 1996; Sakaba et al., 1997b) and electron microscopy analysis (von Gersdorff et al., 1996) have suggested two distinct synaptic vesicle pools that are sequentially depleted: an immediately releasable pool of ~35 fF and a reserve pool of ~120 fF (presumably corresponding to the ~1200 vesicles at the base of all the synaptic ribbons and the ~4800 vesicles attached to the upper four to five rows, respectively). The two components of release may thus correspond to these two morphologically distinct vesicle pools, with all the docked vesicles on the bottom row of the ribbons being fusion competent (Schikorski and Stevens, 1997), in contrast to neuroendocrine cell granules docked at the plasma membrane (Parsons et al., 1995).

The architecture of the synaptic ribbon invites us to suggest that the slower onset kinetics of the second component may reflect the downward movement of vesicles from the upper rows of the synaptic ribbon (reserve pool) to the bottom row where they dock and fuse with the plasma membrane. Interestingly, this mobilization rate is modulated by $Ca^{2+}$ influx, since large $Ca^{2+}$ currents caused the two components of release to fuse together, apparently accelerating the mobilization rate of reserve vesicles toward release sites. Furthermore, sustained $Ca^{2+}$ influx was necessary for the activation of the second component of release (see Figure 5B), suggesting that high levels of submembrane $[Ca]_i$ are necessary for its activation. An alternative mechanism is that there exists a pool of vesicles close to $Ca^{2+}$ channels (first component) and one more distal to $Ca^{2+}$ channels (Neher, 1998), or that there are two $Ca^{2+}$ sensors for vesicle fusion, with low and high affinity for $Ca^{2+}$ (Goda and Stevens, 1994). However, given the rapid onset and offset of release, and the close association of intramembrane particles (putative $Ca^{2+}$ channels; see below) with docked vesicles on the synaptic ribbon, we favor the more economical hypothesis that a single type of low $Ca^{2+}$ affinity sensor triggers vesicle fusion from two morphologically distinct vesicle pools.

**Capacitance Jumps Reflect Glutamate Release**

We have shown a good correlation between capacitance changes and glutamate release and a rapid termination of release after the closure of $Ca^{2+}$ channels. Our dependence of $Q_{Glu}$ on $Q_{Ca}$ shown in Figure 2C is very similar to that reported for conventional active zone synapses formed by amacrine cells, where two components of release are also observed (see Figure 3C of Gleason et al., 1994). However, the short delay in release upon $Ca^{2+}$ current activation and lack of prominent asynchronous release forms an interesting contrast to results in cultured amacrine cells (Gleason et al., 1994), where release can outlast $Ca^{2+}$ current termination by 1–2 s. We have observed no copious asynchronous release for pulses up to 1 s in duration (terminals loaded with 0.2 mM BAPTA; data not shown). Moreover, for terminals loaded with 0.1 mM BAPTA, the high affinity NMDA receptor–mediated response elicited by a 1 s pulse decays back to baseline with the characteristic deactivation time constant of NMDA receptors (~230 ms, Lester et al., 1990; Sakaba et al., 1997b), again indicating that after 1 s long pulses asynchronous release is not copious. However, we emphasize that for pulses of >1 s asynchronous release may become increasingly more significant.

Exocytosis and endocytosis were found to be temporally well separated. For 10 ms depolarizing pulses, the rate of endocytosis ($\tau$ = 1–2 s) is at least 100-fold slower than the decay rate of the first component of exocytosis ($\tau \approx 10$ ms). For 200 ms pulses, the rate of capacitance recovery back to baseline is also fast ($\tau$ = 1–2 s); however, since asynchronous release falls sharply within <300 ms, capacitance jumps elicited by 200 ms pulses to −10 mV should reflect only membrane addition (i.e., exocytosis) and the capacitance recovery only membrane retrieval (i.e., endocytosis). Capacitance measurements have indicated the presence of fast forms of endocytosis in neuroendocrine cells (Neher and Zucker, 1993; Thomas et al., 1994; Artalejo et al., 1995) and pituitary nerve terminals (Hsu and Jackson, 1996). Using fluorescence imaging methods, evidence for fast endocytosis was also recently obtained in hippocampal synaptic boutons (Klingauf et al., 1998). Fast endocytosis may thus be a fairly ubiquitous phenomenon in nerve terminals.

Two components of release were detected, and it is possible that the second component of release may be affected by the kinetics of diffusion and rebinding of glutamate molecules to AMPA receptors in the nonuniform cell-pair gap, or that AMPA receptors undergo two phases of opening during glutamate application (Ishida and Neyton, 1985). However, Eliasof and Jahr (1997) have shown that an 8 ms application of 10 mM glutamate to outside-out patches of catfish horizontal cells treated with CTZ (100 μM) elicits a step-like current, with rapid onset and offset, that was constant throughout the application of glutamate. This nondesensitizing current suggests that these AMPA receptors treated with CTZ are

faithful indicators of glutamate concentration and that the second component is due to a second phase of glutamate release with slower onset kinetics, rather then to diffusional delays and/or rebinding. In addition, we note that in the presence of CTZ whole-cell responses of catfish horizontal cells to glutamate application (10 mM) are not biphasic (Eliasof and Jahr, 1997). Moreover, the good correlation between capacitance jumps and AMPA receptor–mediated responses indicates that the second component of release is due to a second bout of exocytosis. Furthermore, as noted above, a purely "presynaptic" perturbation, loading terminals with 5 mM EGTA or BAPTA, greatly increases the onset time of the second component. Finally, activation of protein kinase C selectively augments the second component (Minami et al., 1998). Taken together, these findings strongly suggest that the second component of release is mediated by a second bout of exocytosis elicited by constant $Ca^{2+}$ influx.

We emphasize also that the AMPA (+ CTZ) -mediated response is not saturated by the amounts of glutamate released in these experiments. Figure 2A, for example, showed that a small $Ca^{2+}$ current elicits a small first component and then a delayed second component, while a larger $Ca^{2+}$ current elicits a larger first component followed by a smaller second component with less delay. However, the integral of the AMPA response and the capacitance jump were the same for both responses, indicating that the amount of release and exocytosis was identical. This again strongly indicates that there are two separate components of release that are modulated by $Ca^{2+}$ influx, rather than the kinetics of $I_{Glu}$ being determined by a putative trapping and/or diffusional delay of transmitter within the cell-pair gap.

Studies in goldfish bipolar cells using FM1-43 have suggested the existence of a continuous mode of release regulated by a high $Ca^{2+}$ affinity ($\sim$1 $\mu$M) sensor for exocytosis (Lagnado et al., 1996). The two components of release we have detected are, however, readily exhaustible. Nevertheless, a continuous recruitment and exocytosis of vesicles may occur for the extremely long (20–400 s) depolarizations to 0 mV used by Lagnado et al. (1996), in which case exocytosis and endocytosis may overlap temporally (Smith and Betz, 1996). Indeed, capacitance jumps elicited by 2 s depolarizing pulses ($\sim$220 fF) are larger than those elicited by 0.25–1 s pulses ($\sim$150 fF), and trains of depolarizations given at 1 Hz lasting 10–15 s can produce even larger cumulative capacitance changes ($\sim$300 fF; von Gersdorff and Matthews, 1997). Low quantal levels of continuous release may also be undetectable at the noise level of our horizontal cell recordings, while the FM1-43 technique may be very sensitive to this continuous release since it integrates signals over several minutes. Alternatively, part of the fluorescence changes detected using FM1-43 could be due to membrane turnover events that are unrelated to glutamate release. We also note that Fura 2 measurements indicate that $[Ca]_i$ remains as high as 0.5–1 $\mu$M for several hundred milliseconds following repolarization from 200 ms pulses that activate currents of the amplitude shown in Figure 5A (Kobayashi and Tachibana, 1995). Nevertheless, no copious asynchronous release was detected, consistent with vesicle pool depletion for pulses longer than 200 ms and a low $Ca^{2+}$ affinity fusion sensor for exocytosis.

### Is the Estimate of $Ca^{2+}$ Channels Reasonable?

The number we estimated of $\sim$5 $Ca^{2+}$ channels per docked vesicle contrasts with similar estimates from a conventional active zone synapse where at least 60 $Ca^{2+}$ channels open per vesicle fusion (Borst and Sakmann, 1996). The brief tail current pulse ($\sim$500 $\mu$s duration) of Figure 4C injected only 0.17 pC of $Ca^{2+}$ ions into the bipolar terminal and elicited a capacitance jump of 24 fF (whereas $C_m$ = 52 fF with Bay-K 8644). This corresponds to $\sim$900 vesicles fusing with the plasma membrane, since the capacitance of a single 29 nm synaptic vesicle is 26.4 aF (von Gersdorff et al., 1996). At a calyx terminal, by contrast, a single action potential injects 0.9 pC of $Ca^{2+}$ ions during $\sim$500 $\mu$s, triggering the fusion of about 200 vesicles (Borst and Sakmann, 1996). Bipolar cell terminals are thus very efficient since they can release reliably a large number of vesicles with rather minimal $Ca^{2+}$ entry. The distinct isoforms of presynaptic proteins expressed at ribbon synapses are beginning to emerge (Morgans et al., 1996) and may endow them with the capacity to fuse large numbers of vesicles rapidly and focally.

Freeze-fracture electron microscopy studies in monkey and rabbit retina show that a total of 100–200 intramembrane particles closely flank the sides of a single bipolar cell synaptic ribbon (Raviola and Raviola, 1982). The particles are 9–11 nm in diameter and lie exclusively within $<$60 nm from vesicle docking sites at the bottom row of the ribbon. En face views of synaptic ribbons show that $\sim$7 vesicles can dock to the plasma membrane on each side of the synaptic ribbon (see inset of Figure 5 of Raviola and Raviola, 1982), for a total of $\sim$14 docked vesicles per ribbon, so there are presumably on average 7–14 particles per docked vesicle. If we further assume that the particles represent $Ca^{2+}$ channels (Pumplin et al., 1981; Roberts et al., 1990) and a smaller proportion of $Ca^{2+}$-dependent $K^+$ channels (Robitaille et al., 1993; Sakaba et al., 1997a), we conclude that the above electrophysiological estimate of $\sim$5 functional $Ca^{2+}$ channels per docked vesicle is quite reasonable. Furthermore, this strategic location of $Ca^{2+}$ channels close to fusion sites explains, within a calcium microdomain concept (Llinás et al., 1995; Schweizer et al., 1995), the weak effects of EGTA (Adler et al., 1991) on the first component of bipolar cell release (Mennerick and Matthews, 1996; Sakaba et al., 1997b). In this regard, it is interesting to also note that while 1 mM EGTA reduces evoked EPSCs to 60% of their initial value in a mammalian conventional active zone synapse (Borst and Sakmann, 1996), concentrations of 5 mM EGTA do not significantly reduce the first component of release (Sakaba et al., 1997b) and capacitance jump (Mennerick and Matthews, 1996; Sakaba et al., 1997b). However, 5–10 mM EGTA does block the second component of release elicited by a 200 ms pulse in bipolar terminals, and long depolarizing pulses (2–3 s) or trains of pulses are necessary to saturate this concentration of buffer and eventually evoke release and capacitance changes (Sakaba et al., 1997b; von Gersdorff and Matthews, 1997).

### Implications for Retinal Signaling

ON-type bipolar cell terminals can thus release relatively large amounts of glutamate on an extremely fast submillisecond time scale. However, this first component of release is exhausted during a 5 ms depolarization to −10 mV. Intracellular sharp electrode recordings from ON-type Mb1 bipolar cells (the class of cells with the giant synaptic terminals we have used here) show that in dark-adapted retina light flashes can rapidly depolarize the cells from a resting potential of −40 mV to −10 mV (Saito et al., 1979). The first component of release we have described here may thus serve to transmit information about rapidly changing levels of light intensity (high frequency signals), while the second component (counteracting premature depletion of a readily releasable pool) is used to transmit more sustained visual input (low frequency signals). Indeed, bipolar cells provide excitatory input to ganglion cells that are capable of faithfully following flickering light flashes to frequencies of up to 60 Hz (Fukada and Saito, 1971; Lee, 1996). It is possible that the rapid onset and offset of release we report here, from a particular class of bipolar cell, allows the retina to perform this task. Our results also suggest that transient responses to light in amacrine and ganglion cells (Werblin and Dowling, 1969; Kaneko, 1970; Taylor et al., 1995) can be partly due to the intrinsic properties of phasic release from bipolar terminals. Other mechanisms, such as postsynaptic receptor desensitization, $I_{Ca}$ inactivation, and negative feedback via reciprocal inhibitory synapses, may also contribute to further sharpen the transient nature of ON–OFF responses (Dacheux and Raviola, 1986; Dixon and Copenhagen, 1992; Roska et al., 1998). The phasic nature of release at bipolar cell terminals is also consistent with the view that bipolar cells function as electrical bandpass filters with differentiating properties (Baylor and Fettiplace, 1977).

Bipolar cell ribbons thus contrast in their kinetics and capacity of release with the much larger ribbons (or dense bodies) of hair cells (Parsons et al., 1994) and photoreceptors (Rieke and Schwartz, 1996), where capacitance changes do not saturate within 200 ms of strong stimulation. Differences in releasable pool size and mobilization rates of vesicles on and toward ribbons may account for this. In addition, transmission to the postsynaptic cells will also depend critically on the degree of desensitization of AMPA receptors. It is interesting to note that dopamine levels in the retina can change drastically during light adaptation, and dopamine alters the desensitization rate of some retinal AMPA receptors (Knapp and Dowling, 1987; Schmidt et al., 1994).

### Experimental Procedures

#### Cell Isolation

Dissociated goldfish (*Carassius auratus*) bipolar cell terminals (~10 μm in diameter, Mb1 ON-type; Sherry and Yazulla, 1993) and 1- to 4-day-old cultured catfish (*Ictalurus punctatus*) horizontal cells were prepared as previously described (Tachibana et al., 1993). Pieces of retina were treated with hyaluronidase (5 min) followed by papain (10–20 min, 28°C) and mechanical trituration with pipettes. Isolated cells were allowed to settle on the bottom of the recording chamber for 5–10 min and were then superfused continuously at a rate of 0.3–0.5 ml/min. Terminals were identified by their size, bulbous shape (often with a short axon stump) and characteristic calcium current. All terminal recordings were done within <3 hr after dissociation. The recording solution (~22°C) contained (in mM) 125 NaCl, 2.6 KCl, 2.5 $CaCl_2$, 1 $MgCl_2$, 10 glucose, 10 HEPES (pH 7.4, 270 mOsm), and 0.1 mg/ml bovine serum albumin (Sigma). After establishing a cell pair, the recording solution was supplemented with 10 μM glycine, 2 μM strychnine, 100 μM CTZ (dissolved in DMSO), and 50 μM D-AP5, unless otherwise indicated, and rapidly applied onto cells via a Y-tube microflow system (Tachibana et al., 1993), which was placed in the vicinity of the cell pair. The final DMSO concentration was 0.1%. Catfish horizontal cells express both non-NMDA and NMDA receptors (O'Dell and Christensen, 1989), but we found that the non-NMDA (AMPA) receptor–mediated current tended to slowly decrease in size with days in culture.

#### Patch-Clamp Recordings

The bipolar terminal patch pipette solution contained (in mM) 50 Cs-gluconate, 40–50 Cs-glutamate, 10 CsCl, 10 TEA-Cl, 0.2 BAPTA, 5.5 $MgCl_2$, 5 ATP-$Na_2$, 0–0.5 GTP, and 30 HEPES (pH 7.2 with CsOH, 270 mOsm). Horizontal cell patch pipette solution contained (in mM) 110 CsCl, 10 TEA-Cl, 5 EGTA, 0.5 $CaCl_2$, 5.5 $MgCl_2$, 5 ATP-$Na_2$, 0–0.5 CsF, 0.5 cAMP, and 20–30 HEPES (pH 7.2 with CsOH). Conventional whole-cell mode patch-clamp recordings were performed with EPC−9 and EPC−7 patch-clamp amplifiers (Heka). The EPC−9 was controlled by Pulse (Heka) software run on a Macintosh Quadra computer. Capacitance measurements were made in the "sine+DC" mode of the EPC−9 software emulation lock-in amplifier, with an 800–1200 Hz sine wave (30 mV peak-to-peak) applied on a −60 mV holding potential (Gillis, 1995). Depending on the depolarizing pulse duration, $C_m$ data points were calculated by averaging over 8–32 cycles of the sine wave. For all capacitance traces, analyzed series resistance ($R_s$) changes did not correlate with $C_m$ changes. Bipolar terminal $R_s$ and initial capacitance were 12–35 MΩ and 1.8–4.5 pF. Horizontal cell $R_s$ and initial capacitance were 8–30 MΩ and 28–54 pF. Horizontal cell $R_s$ was compensated 40%–50%. Generally, horizontal cells were held at −70 mV. Liquid junction potential was not corrected. The time interval between evoked responses was 30–50 s to allow for complete recovery of responses from depression. Currents were low-pass filtered online at 5–16 kHz and sampled at 10–200 μs depending on the voltage-clamp pulse duration used. Bipolar leak currents (<40 pA) were measured by 3.5 mM $Co^{2+}$ substitution of $Ca^{2+}$ and $Mg^{2+}$. $Ca^{2+}$ tail current data was filtered at 10–16 kHz and sampled at 10–24 μs and series resistance compensated from 50%–80% (10 μs delay), so that voltage-clamp speed ($R_s \times C_m$) was 20–40 μs. Offline analysis and low-pass filtering of data at 150–500 Hz were done using Pulse+Xchart (Heka) and IgorPro software (Wavemetrics).

#### Acknowledgments

We thank Erwin Neher for comments on the manuscript and continuous support, Gary Matthews, Aaron Fox and Heinz Wässle for discussions, and Haruo Kasai and Erwin Neher for the loan of equipment. This work was supported by the Ministry of Education, Science, Sports and Culture of Japan (M. T.) and the Human Frontier Science Program (H. v. G.).

Received July 14, 1998; revised October 9, 1998.

#### References

Adler, E.M., Augustine, G.J., Duffy, S.N., and Charlton, M.P. (1991). Alien intracellular calcium chelators attenuate neurotransmitter release at the squid giant synapse. J. Neurosci. *11*, 1496–1507.

Albillos, A., Dernick, G., Horstmann, H., Almers, W., Alvarez de Toledo, G., and Lindau, M. (1997). The exocytotic event in chromaffin cells revealed by patch amperometry. Nature *389*, 509–512.

Artalejo, C.R., Henley, J.R., McNiven, M.A., and Palfrey, C.H. (1995). Rapid endocytosis coupled to exocytosis in adrenal chromaffin cells involves $Ca^{2+}$, GTP, and dynamin but not clathrin. Proc. Natl. Acad. Sci. USA *92*, 8328–8332.

Augustine, G.J. (1990). Regulation of transmitter release at the squid

giant synapse by presynaptic delayed rectifier potassium current. J. Physiol. *431*, 343–364.

Augustine, G.J., Charlton, M.P., and Smith, S.J. (1985). Calcium entry and transmitter release at voltage-clamped nerve terminals of squid. J. Physiol. *369*, 163–181.

Barrett, E.F., and Stevens, C.F. (1972). The kinetics of transmitter release at the frog neuromuscular junction. J. Physiol. *227*, 691–708.

Baylor, D.A., and Fettiplace, R. (1977). Kinetics of synaptic transfer from receptors to ganglion cells in turtle retina. J. Physiol. *271*, 425–448.

Borst, J.G.G., and Sakmann, B. (1996). Calcium influx and transmitter release in a fast CNS synapse. Nature *383*, 431–434.

Chow, R.H., Klingauf, J., Heinemann, C., Zucker, R.S., and Neher, E. (1996). Mechanisms determining the time course of secretion in neuroendocrine cells. Neuron *16*, 369–376.

Church, P.J., and Stanley, E.F. (1996). Single L-type calcium channel conductance with physiological levels of calcium in chick ciliary ganglion neurons. J. Physiol. *496*, 59–68.

Copenhagen, D.R., and Jahr, C.E. (1989). Release of endogenous excitatory amino acids from turtle photoreceptors. Nature *341*, 536–539.

Cousin, M.A., and Nicholls, D.G. (1997). Synaptic vesicle recycling in cultured cerebellar granule cells: role of vesicular acidification and refilling. J. Neurochem. *69*, 1927–1935.

Dacheux, R.F., and Raviola, E. (1986). The rod pathway in the rabbit retina: a depolarizing bipolar and amacrine cell. J. Neurosci. *6*, 331–345.

De Camilli, P., and Takei, K. (1996). Molecular mechanisms in synaptic vesicle endocytosis and recycling. Neuron *16*, 481–486.

de Ruyter van Steveninck, R.R, and Laughlin, S.B. (1996). The rate of information transfer at graded-potential synapses. Nature *379*, 642–645.

Diamond, J.S., and Jahr, C.E. (1995). Asynchronous release of synaptic vesicles determines the time course of the AMPA receptor–mediated EPSC. Neuron *15*, 1097–1107.

Dixon, D.B., and Copenhagen, D.R. (1992). Two types of glutamate receptors differentially excite amacrine cells in the tiger salamander retina. J. Physiol. *449*, 589–606.

Eliasof, S., and Jahr, C.E. (1997). Rapid AMPA receptor desensitization in catfish cone horizontal cells. Vis. Neurosci. *14*, 13–18.

Elmquist, D., and Quastel, D. (1965). A quantitative study of endplate potentials in isolated human muscle. J. Physiol. *178*, 505–529.

Fox, A.P., Nowycky, M.C., and Tsien, R.W. (1987). Single-channel recordings of three types of calcium channels in chick sensory neurones. J. Physiol. *394*, 173–200.

Fukada, Y., and Saito, H.-A. (1971). The relationship between response characteristics to flicker stimulation and receptive field organization in the cat's optic nerve fibers. Vision Res. *11*, 227–240.

Geiger, J.R.P., Lübke, J., Roth, A., Frotscher, M., and Jonas, P. (1997). Submillisecond AMPA receptor–mediated signaling at a principal neuron–interneuron synapse. Neuron *18*, 1009–1023.

Gillis, K. (1995). Techniques for membrane capacitance measurements. In Single-Channel Recording, Second Edition, B. Sakmann and E. Neher, eds. (New York: Plenum Press), pp. 155–198.

Gleason, E., Borges, S., and Wilson, M. (1994). Control of transmitter release from retinal amacrine cells by $Ca^{2+}$ influx and efflux. Neuron *13*, 1109–1117.

Goda, Y., and Stevens, C.F. (1994). Two components of transmitter release at a central synapse. Proc. Natl. Acad. Sci. USA *91*, 12942–12946.

Heidelberger, R. (1998). Adenosine triphosphate and the late steps in calcium-dependent exocytosis at a ribbon synapse. J. Gen. Physiol. *111*, 225–241.

Heidelberger, R., Heinemann, C., Neher, E., and Matthews, G. (1994). Calcium dependence of the rate of exocytosis in a synaptic terminal. Nature *371*, 513–515.

Henkel, A.W., and Almers, W. (1996). Fast steps in exocytosis and endocytosis studied by capacitance measurements in endocrine cells. Curr. Opin. Neurobiol. *6*, 350–357.

Heuser, J.E., and Reese, T.S. (1981). Structural changes after transmitter release at the frog neuromuscular junction. J. Cell Biol. *88*, 564–580.

Hsu, S.-F., and Jackson, M.B. (1996). Rapid exocytosis and endocytosis in nerve terminals of the rat posterior pituitary. J. Physiol. *494*, 539–553.

Isaacson, J.S., and Walmsey, B. (1995). Counting quanta: direct measurements of transmitter release at a central synapse. Neuron *15*, 875–884.

Ishida, A.T., and Neyton, J. (1985). Quisqualate and L-glutamate inhibit retinal horizontal-cell responses to kainate. Proc. Natl. Acad. Sci. USA *82*, 1837–1841.

Kaneko, A. (1970). Physiological and morphological identification of horizontal, bipolar and amacrine cells in goldfish retina. J. Physiol. *207*, 623–633.

Katz, B., and Miledi, R. (1965). The measurement of synaptic delay, and the time course of acetylcholine release at the neuromuscular junction. Proc. R. Soc. Lond. B Biol. Sci. *161*, 483–495.

Klingauf, J., Kavalali, E.T., and Tsien, R.W. (1998). Kinetics and regulation of fast endocytosis at hippocampal synapses. Nature *394*, 581–585.

Knapp, A.G., and Dowling, J.E. (1987). Dopamine enhances excitatory amino acid–gated conductances in cultured retinal horizontal cells. Nature *325*, 437–439.

Kobayashi, K., and Tachibana, M. (1995). $Ca^{2+}$ regulation in the presynaptic terminals of goldfish retinal bipolar cells. J. Physiol. *483*, 79–94.

Lagnado, L., Gomis, A., and Job, C. (1996). Continuous vesicle cycling in the synaptic terminal of retinal bipolar cells. Neuron *17*, 957–967.

Lando, L., and Zucker, R.S. (1994). $Ca^{2+}$ cooperativity in neurosecretion measured using photolabile $Ca^{2+}$ chelators. J. Neurophysiol. *72*, 825–830.

Lee, B.B. (1996). Receptive field structure in the primate retina. Vision Res. *36*, 631–644.

Lester, R.A.J., Clements, J.D., Westbrook, G.L., and Jahr, C.E. (1990). Channel kinetics determine the time course of NMDA receptor–mediated synaptic currents. Nature *346*, 565–567.

Liu, G., and Tsien, R.W. (1995). Properties of synaptic transmission at single hippocampal synaptic boutons. Nature *375*, 404–408.

Llinás, R., Steinberg, I.Z., and Walton, K. (1981). Relationship between presynaptic calcium current and postsynaptic potential in squid giant synapse. Biophys. J. *33*, 323–352.

Llinás, R., Sugimori, M., and Silver, R.B. (1995). The concept of calcium concentration microdomains in synaptic transmission. Neuropharmacology *34*, 1443–1451.

Lukasiewicz, P.D., Lawrence, J.E., and Valentino, T.L. (1995). Desensitizing glutamate receptors shape excitatory synaptic inputs to tiger salamander retinal ganglion cells. J. Neurosci. *15*, 6189–6199.

Mennerick, S., and Matthews, G. (1996). Ultrafast exocytosis elicited by calcium current in synaptic terminals of retinal bipolar neurons. Neuron *17*, 1241–1249.

Mennerick, S., and Zorumski, C.F. (1995). Paired-pulse modulation of fast excitatory synaptic currents in microcultures of rat hippocampal neurons. J. Physiol. *488*, 85–101.

Minami, N., Berglund, K., Sakaba, T., Kohmoto, H., and Tachibana, M. (1998). Potentiation of transmitter release by protein kinase C in goldfish retinal bipolar cells. J. Physiol. *521*, 219–225.

Morgans, C.W., Brandstätter, J.H., Kellerman, J., Betz, H., and Wässle, H. (1996). A SNARE complex containing syntaxin 3 is present in ribbon synapses of the retina. J. Neurosci. *16*, 6713–6721.

Moser, T., and Neher, E. (1997). Estimation of the mean exocytic vesicle capacitance in mouse adrenal chromaffin cells. Proc. Natl. Acad. Sci. USA *94*, 6735–6740.

Naraghi, M., and Neher, E. (1997). Linearized buffered $Ca^{2+}$ diffusion in microdomains and its implications for calculation of $[Ca^{2+}]$ at the mouth of a calcium channel. J. Neurosci. *17*, 6961–6973.

Neher, E. (1998). Vesicle pools and $Ca^{2+}$ microdomains: new tools for understanding their roles in neurotransmitter release. Neuron *20*, 389–399.

Neher, E., and Marty, A. (1982). Discrete changes of cell capacitance observed under conditions of enhanced secretion in bovine adrenal chromaffin cells. Proc. Natl. Acad. Sci. USA *79*, 6712–6716.

Neher, E., and Zucker, R.S. (1993). Multiple calcium-dependent processes related to secretion in bovine chromaffin cells. Neuron *10*, 21–30.

Nowycky, M.C., Fox, A.P., and Tsien, R.W. (1985). Long-opening mode of gating of neuronal calcium channels and its promotion by the dihydropyridine calcium agonist Bay K 8644. Proc. Natl. Acad. Sci. USA *82*, 2178–2182.

O'Dell, T.J., and Christensen, B.N. (1989). Horizontal cells isolated from catfish retina contain two types of excitatory amino acid receptors. J. Neurophysiol. *61*, 1097–1109.

Okada, T., Horiguchi, H., and Tachibana, M. (1995). $Ca^{2+}$-dependent $Cl^-$ current at the presynaptic terminals of goldfish retinal bipolar cells. Neurosci. Res. *23*, 297–303.

Parsons, T.D., Lenzi, D., Almers, W., and Roberts, W.M. (1994). Calcium-triggered exocytosis and endocytosis in an isolated presynaptic cell: capacitance measurements in saccular hair cells. Neuron *13*, 875–883.

Parsons, T.D., Coorssen, J.R., Horstmann, H., and Almers, W. (1995). Docked granules, the exocytic burst, and the need for ATP hydrolysis in endocrine cells. Neuron *15*, 1085–1096.

Partin, K.M., Patneau, D.K., Winters, C.A., Mayer, M.L., and Buonanno, A. (1993). Selective modulation of desensitization at AMPA versus kainate receptors by cyclothiazide and concanavalin A. Neuron *11*, 1069–1082.

Pumplin, D.W., Reese, T.S., and Llinás, R. (1981). Are the presynaptic membrane particles the calcium channels? Proc. Natl. Acad. Sci. USA *78*, 7210–7213.

Raviola, E., and Raviola, G. (1982). Structure of synaptic membranes in the inner plexiform layer of the retina: a freeze-fracture study in monkeys and rabbits. J. Comp. Neurol. *209*, 233–248.

Rieke, F., and Schwartz, E.A. (1996). Asynchronous transmitter release: control of exocytosis and endocytosis at the salamander rod synapse. J. Physiol. *493*, 1–8.

Roberts, W.M., Jacobs, R.A., and Hudspeth, A.J. (1990). Colocalization of ion channels involved in frequency selectivity and synaptic transmission at presynaptic active zones of hair cells. J. Neurosci. *10*, 3664–3684.

Robitaille, R., Garcia, M.L., Kaczorowski, G.J., and Charlton, M.P. (1993). Functional colocalization of calcium and calcium-gated potassium channels in control of transmitter release. Neuron *11*, 645–655.

Rosenmund, C., and Stevens, C.F. (1996). Definition of the readily releasable pool of vesicles at hippocampal synapses. Neuron *16*, 1197–1207.

Roska, B., Nemeth, E., and Werblin, F.S. (1998). Response to change is facilitated by a three-neuron disinhibitory pathway in the tiger salamander retina. J. Neurosci. *18*, 3451–3459.

Ryan, T.A., Smith, S.J., and Reuter, H. (1996). The timing of synaptic vesicle endocytosis. Proc. Natl. Acad. Sci. USA *93*, 5567–5571.

Sabatini, B., and Regehr, W. (1996). Timing of neurotransmission at fast synapses in the mammalian brain. Nature *384*, 170–172.

Saito, T., Kondo, H., and Toyoda, J.-I. (1979). Ionic mechanisms of two types of ON-center bipolar cells in the carp retina. J. Gen. Physiol. *73*, 73–90.

Sakaba, T., Ishikane, H., and Tachibana, M. (1997a). $Ca^{2+}$-activated $K^+$ current at presynaptic terminals of goldfish retinal bipolar cells. Neurosci. Res. *27*, 219–228.

Sakaba, T., Tachibana, M., Matsui, K., and Minami, N. (1997b). Two components of transmitter release in retinal bipolar cells: exocytosis and mobilization of synaptic vesicles. Neurosci. Res. *27*, 357–370.

Schikorski, T., and Stevens, C.F. (1997). Quantitative ultrastructural analysis of hippocampal excitatory synapses. J. Neurosci. *17*, 5858–5867.

Schmidt, K.F., Kruse, M., and Hatt, H. (1994). Dopamine alters glutamate receptor desensitization in retinal horizontal cells of the perch (*perca fluviatilis*). Proc. Natl. Acad. Sci. USA *91*, 8288–8291.

Schweizer, F.E., Betz, H., and Augustine, G.J. (1995). From vesicle docking to endocytosis: intermediate reactions of exocytosis. Neuron *14*, 689–696.

Sherry, D.M., and Yazulla, S. (1993). Goldfish bipolar cells and axon terminal patterns: a Golgi study. J. Comp. Neurol. *329*, 188–200.

Simon, S.M., and Llinás, R. (1985). Compartmentalization of the submembrane calcium activity during Ca influx and its significance in transmitter release. Biophys. J. *48*, 485–498.

Smith, C.B., and Betz, W.J. (1996). Simultaneous independent measurement of endocytosis and exocytosis. Nature *380*, 531–534.

Song, H.-J., Ming, G.-L., Fon, E., Bellocchio, E., Edwards, R.H., and Poo, M.-M. (1997). Expression of a putative vesicular acetylcholine transporter facilitates quantal transmitter packaging. Neuron *18*, 815–826.

Spencer, A.N., Przysiezniak, J., Acosta-Urquidi, J., and Basarsky, T.A. (1989). Presynaptic spike broadening reduces junctional potential amplitude. Nature *340*, 636–638.

Stanley, E.F. (1993). Single calcium channels and acetylcholine release at a presynaptic nerve terminal. Neuron *11*, 1007–1011.

Stevens, C.F., and Wang, Y. (1995). Facilitation and depression at single central synapses. Neuron *14*, 795–802.

Steyer, J.A., Horstmann, H., and Almers, W. (1997). Transport, docking and exocytosis of single secretory granules in live chromaffin cells. Nature *388*, 474–478.

Tachibana, M., Okada, T., Arimura, T., Kobayashi, K., and Piccolino, M. (1993). Dihydropyridine-sensitive calcium current mediates neurotransmitter release from bipolar cells of the goldfish retina. J. Neurosci. *13*, 2898–2909.

Taylor, W.R., Chen, E., and Copenhagen, D.R. (1995). Characterization of spontaneous excitatory synaptic currents in salamander retinal ganglion cells. J. Physiol. *486*, 207–221.

Thomas, P., Lee, A.K., Wong, G.J., and Almers, W. (1994). A triggered mechanism retrieves membrane in seconds after $Ca^{2+}$-stimulated exocytosis in single pituitary cell. J. Cell Biol. *124*, 667–675.

Trussell, L.O., and Fischbach, G.D. (1989). Glutamate receptor desensitization and its role in synaptic transmission. Neuron *3*, 209–218.

Vincent, P., and Marty, A. (1996). Fluctuations of inhibitory postsynaptic currents in Purkinje cells from rat cerebellar slices. J. Physiol. *494*, 183–199.

von Gersdorff, H., and Matthews, G. (1997). Depletion and replenishment of vesicle pools at a ribbon-type synaptic terminal. J. Neurosci. *17*, 1919–1927.

von Gersdorff, H., Vardi, E., Matthews, G., and Sterling, P. (1996). Evidence that vesicles on the synaptic ribbon of retinal bipolar neurons can be rapidly released. Neuron *16*, 1221–1227.

von Rüden, L., and Neher, E. (1993). A Ca-dependent early step in the release of catecholamines from adrenal chromaffin cells. Science *262*, 1061–1065.

Werblin, F.S., and Dowling, J.E. (1969). Organization of the retina of the mudpuppy, *Necturus maculosus*. II. Intracellular recording. J. Neurophysiol. *32*, 339–355.

Wu, L.-G., and Betz, W.J. (1996). Nerve activity but not intracellular calcium determines the time course of endocytosis at the frog neuromuscular junction. Neuron *17*, 769–779.

Yamada, K.A., and Tang, C.-M. (1993). Benzothiazides inhibit rapid glutamate receptor desensitization and enhance glutamatergic synaptic currents. J. Neurosci. *13*, 3904–3915.

Yazejian, B., DiGregorio, D.A., Vergara, J.L., Poage, R.E., Meriney, S.D., and Grinnell, A.D. (1997). Direct measurements of presynaptic calcium and calcium-activated potassium currents regulating neurotransmitter release at cultured *Xenopus* nerve–muscle synapses. J. Neurosci. *17*, 2990–3001.

Zucker, R.S., and Fogelson, A.L. (1986). Relationship between transmitter release and presynaptic calcium influx when calcium enters through discrete channels. Proc. Natl. Acad. Sci. *83*, 3032–3036.